

RESEARCH ARTICLE | MAY 29 2025

Effect of the repeated application of First Contact™ polymer on xenon-difluoride passivated lithium fluoride on aluminum surfaces for space telescopes

Special Collection: [Papers from the AVS 70th International Symposium](#)

Joshua Vawdrey   ; James Hamilton  ; Drew Watson  ; Lauren Miner  ; Osemudiamhen Destiny Amienghemhen  ; Walter Paxton  ; David Allred 



J. Vac. Sci. Technol. A 43, 043408 (2025)

<https://doi.org/10.1116/6.0004601>

 CHORUS



Articles You May Be Interested In

Surface etching of YBCO films by xenon difluoride

J. Vac. Sci. Technol. B (July 2005)

EXAFS and XPS Study of Rutile-Type Difluorides of First-Row Transition Metals

AIP Conf. Proc. (February 2007)

Si-based materials for lithium-ion batteries X: 70% surface-modified Si/C/polyvinylidene difluoride-carbon black/lithiated polyacrylic acid electrode

Surf. Sci. Spectra (May 2020)

04 June 2025 14:57:01



Instruments for Advanced Science



- Knowledge
- Experience
- Expertise

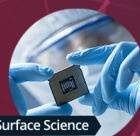
[Click to view our product catalogue](#)

Contact Hiden Analytical for further details:
 www.HidenAnalytical.com
 info@hiden.co.uk



Gas Analysis

- ▶ dynamic measurement of reaction gas streams
- ▶ catalysis and thermal analysis
- ▶ molecular beam studies
- ▶ dissolved species probes
- ▶ fermentation, environmental and ecological studies



Surface Science

- ▶ UHV TPD
- ▶ SIMS
- ▶ end point detection in ion beam etch
- ▶ elemental imaging - surface mapping



Plasma Diagnostics

- ▶ plasma source characterization
- ▶ etch and deposition process reaction kinetic studies
- ▶ analysis of neutral and radical species



Vacuum Analysis

- ▶ partial pressure measurement and control of process gases
- ▶ reactive sputter process control
- ▶ vacuum diagnostics
- ▶ vacuum coating process monitoring

Effect of the repeated application of First Contact™ polymer on xenon-difluoride passivated lithium fluoride on aluminum surfaces for space telescopes

Cite as: J. Vac. Sci. Technol. A 43, 043408 (2025); doi: 10.1116/6.0004601

Submitted: 26 March 2025 · Accepted: 8 May 2025 ·

Published Online: 29 May 2025



View Online



Export Citation



CrossMark

Joshua Vawdrey,^{1,a)} James Hamilton,^{2,3} Drew Watson,⁴ Lauren Miner,¹ Osemudiamhen Destiny Amienghemhen,⁵ Walter Paxton,⁵ and David Allred¹

AFFILIATIONS

¹Department of Physics and Astronomy, BYU College of Computational, Mathematical, and Physical Sciences, Brigham Young University, N284 ESC, Provo, Utah 84602

²Department of Chemistry, University of Wisconsin-Platteville, Platteville, Wisconsin 53818

³Photonic Cleaning Technologies, Platteville, Wisconsin 53818

⁴Rose-Hulman Institute of Technology, Terre Haute, Indiana 47803

⁵Department of Chemistry, BYU College of Computational, Mathematical, and Physical Sciences, Brigham Young University, Provo, Utah 84602

Note: This paper is part of the Special Topic Collection: Papers from the AVS 70th International Symposium.

Author to whom correspondence should be addressed: jvaw94@gmail.com

ABSTRACT

The far-UV (FUV) reflectance of the state-of-the-art, broadband UV/optical/IR mirrors of XeF₂-passivated LiF on Al (Al + XeLiF) is promising for future space telescope missions. To reach their potential, dependable cleaning procedures and storage methods for such reflective surfaces need to be developed. First Contact™ polymer (FCP) formulations have proven to be a reliable method for cleaning conventional mirror surfaces coated with oxides or bare metal and for protecting them in storage. We report here on studies of the cleaning and storage of Al + XeLiF samples using customized FCP formulations designed by Photonic Cleaning Technologies. Cleaning of such mirrors is demanding since fluoride coatings are softer than oxides and can be moisture sensitive. Any damage that marks the overcoat can lead to catastrophic loss of FUV reflectance due to surface roughening and formation of aluminum oxide, which is FUV opaque. We discovered that one formulation could be successfully applied to and removed from Al + XeLiF coatings multiple times. The coatings retained low roughness, minimal aluminum oxide thickness, and high far-UV reflectance. Another of the four FCP formulations successfully cleaned the Al + XeLiF coatings several times. Variable-angle, spectroscopic ellipsometry, tapping-mode atomic force microscopy, x-ray photoelectron spectroscopy, and FUV reflectance allowed us to observe any changes in reflectance and surface roughness, the formation of aluminum oxide, and damage to coating integrity. From the studies of the range of FCP-fluoride interactions, we noted that too much polymer-to-surface adhesion or exposure to trace water in the polymer can result in coating damage.

Published under an exclusive license by the AVS. <https://doi.org/10.1116/6.0004601>

I. INTRODUCTION

The Hubble Space Telescope was predicted to have less than 10% loss of throughput due to contamination from ground-based operations and launch.¹ To mitigate reflectance losses from

contaminants for space missions, contamination budgets are often established based on specific objectives.² Space telescope mirrors for far-UV (FUV) applications are typically composed of aluminum with a metal fluoride thin-film passivation layer with a high

bandgap—such as MgF_2 or LiF —capping layer to mitigate oxidation that can reduce far-UV reflectance.^{3,4} A leading candidate coating for the mirrors for the in-development NASA space telescope mission Habitable Worlds Observatory (HWO) is rPVD XeF_2 -passivated LiF on Al ($\text{Al} + \text{XeLiF}$).^{5–10} It also comes with a challenge: LiF is hygroscopic and is slightly soluble in water, which in humid environments leads to recrystallization of the smooth, conformational LiF layer into larger grains that can leave the aluminum film layer unprotected.^{7–9} In addition, $\text{Al} + \text{XeLiF}$ has been shown via atomic force microscopy (AFM) and SEM to roughen in humid environments and swell under electron bombardment.^{7–10} Due to capillary action, defects and pores in the LiF layer may lead water into the Al layer, oxidizing the Al and forming amorphous alumina (assumed as Al_2O_3) that substantially reduces the far-UV reflectivity.^{7–9} These difficulties require cleaning to not only remove contaminants down to the angstrom level but also not significantly alter the surface of $\text{Al} + \text{XeLiF}$ mirrors and degrade specular reflectance.

One such cleaning method involves using dry-peel First Contact™ Polymer (FCP), a proprietary blend of polymers and solvents developed by Photonic Cleaning Technologies. FCP has been shown to clean optical surfaces down to the angstrom level without causing surface damage or leaving residue.¹¹ FCP is actively used for large-scale optical projects such as LIGO to clean and protect surfaces from contamination.¹² To mitigate unintended polymer-surface interactions such as surface damage, formulations tailored for complex or fragile surfaces have been developed. Gold coatings, for example, are especially fragile and require less adhesion than the standard formulation to limit the potential surface damage. Similarly, fluorides, in general, and LiF , in particular, are complex surfaces to clean and protect from contaminants due to their hygroscopic nature. Absorbed water at the surface is thought to be associated with grain growth in the LiF layer, leading to thin spots and holes in this barrier coating. This enables water and air to come into contact with Al .^{7–9} These lead to Al oxidation, which drastically reduces far-UV reflectance.

The case has been advanced that there are unique astrophysical phenomena in the Lyman UV between the Lyman limit (91.2 nm) and H Lyman- α (121.6 nm).¹³ One objective HWO has is to characterize astrophysical phenomena down to the Lyman- β (102.6 nm). The high far-UV reflectance (above 50% from 100 to 120 nm and above 80% from 120 to 190 nm)⁶ and high reflectance in the near UV, optical, and IR bands are key features of $\text{Al} + \text{XeLiF}$.¹⁴ $\text{Al} + \text{XeLiF}$ has two characteristics that are important for HWO reaching its objectives: its far-UV reflectance and low surface roughness.¹⁴ However, the hygroscopic nature of materials such as LiF could jeopardize mirror performance by allowing aluminum oxide (we use Al_2O_3 to stand for any form of aluminum oxide including hydroxides) to form. It is highly absorptive in the far-UV. Therefore, the FCP formulation used should not encourage the formation of Al_2O_3 . A lack of increased surface roughening typically characterized as root mean square (RMS) roughness would also be an indicator for the success of an FCP formulation on $\text{Al} + \text{XeLiF}$. The HWO mirror requires <1 nm RMS roughness for proper coronagraph functionality.¹⁵ Possible residual surface features from FCP-application, such as polymer residuals (if they occurred), coalesced LiF clumps, or debris, could reduce the

achieved coronagraph contrast and disrupt the detection of terrestrial exoplanets around their stars. Surface clearers, such as FCP, must be thoroughly tested on $\text{Al} + \text{XeLiF}$ to understand polymer-surface interactions including Al oxidation and surface-feature formation.

In this study, we hypothesized that one or more of the formulations belonging to the FCP family would be able to clean particulate contaminants on the mirror due to their success on other surfaces. From the formulations of the current FCP, the following concerns were advanced and were tested to determine their validity or to eliminate them as concerns: (1) While the surface efficacy of the media would be high, trace amounts of water in the formulation could potentially promote Al oxidation in light of LiF 's hygroscopic nature and (2) LiF could potentially swell due to water in the FCP or (3) might sustain damage due to over strong adhesion to the polymer. All three concerns represent considerations for single and repeated FCP-applications.

To test these concerns and characterize the changes $\text{Al} + \text{XeLiF}$ experiences with single and repeated FCP-applications, variable-angle, spectroscopic ellipsometry (VASE) is employed as the workhorse technique. VASE consists of reflecting white light that is linearly polarized 45° from the s - and p -planes. As the light reflects, the polarization changes can be characterized by $\tan \Psi e^{i\Delta} = r_p/r_s$, where the ratio of the Fresnel coefficients r_p/r_s in the p and s directions is related to Ψ (amplitude) and Δ (phase).¹⁶ A multivariable model is then used to fit atomic thicknesses of the thin-film stack that corresponds to the experimental Ψ and Δ values, with CompleteEase™'s generated mean square error indicating the fit quality. To limit degeneracies between parameters, selected collated parameters were constrained in the fit by other physical observations and inputs. For example, surface roughness can also be determined via AFM and was used to identify surface features and analyze trends in the RMS nanoroughness.

II. EXPERIMENT

A. Sample preparation

$\text{Al} + \text{XeLiF}$ was deposited on a Si wafer, (100) orientation, at NASA-GSFC 7 months prior to the start of our experiment and the wafer shipped to BYU 3 months prior. The samples were transported from GSFC to the lab in a specially prepared container that was backfilled with inert gas. Samples ($\sim 1 \times 1 \text{ in.}^2$) were cleaved from the wafer. Then, they and the remaining wafer pieces were stored in a desiccator [$<10\%$ – 18% relative humidity (RH)] until the experiments began. During the measurement process, we kept the wafer pieces in two 3 in. diameter Fluoroware® polypropylene wafer carriers face up. One wafer piece—the control—was kept in one of the 3 in. diameter wafer carriers face up as well with no FCP applied to it. For the latter half of the experiment, the pieces were held down with a double-stick tape on the bottom of the wafer. In the cases that the wafer pieces came unstuck, we would ensure that they were returned back to their original position so they would not slide across each other during transport to the ellipsometer. As shown in Fig. 1, as determined by ellipsometry, Al was around 25 nm thick and the LiF was around 14 nm but varied slightly from sample to sample as expected for evaporated films where special efforts are not expended to ensure thickness uniformity. As part of

04 June 2025 14:57:01

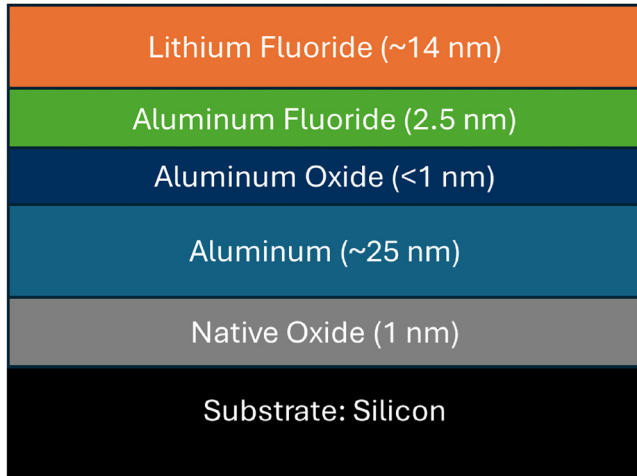


FIG. 1. Model of the thin-film stack of the thin Al + XeLiF used in this study. Al is deposited by evaporation and AlF_3 is formed from a XeF_2 -passivation process. Without breaking vacuum, LiF is deposited by evaporation afterward as a capping layer.

the stack deposition process, the *in situ* XeF_2 -passivation process produces a 2-to-3 nm AlF_3 layer on the evaporated aluminum layer. Due to how the Al + XeLiF is deposited, the fluorides are exceptionally smooth and conformal and are seen to be an effective barrier to oxidation under normal laboratory conditions.^{7,8} An aluminum oxide layer under AlF_3 is not expected due to fluorine displacing any surface oxide in the deposition process. It was certainly less than 1 nm thick. Note that by design Al was deliberately made about 70% thinner than is used in actual Al mirrors. Under such conditions, the ellipsometer's light could penetrate the Al film and reflect off the entirety of the optical stack. This aids in constraining layer thicknesses in the model.

In this study, we define a “peel-off” as a process consisting of the following steps: (1) Applying a specific FCP formulation on the surface of Al + XeLiF, (2) removing the FCP layer by embedding chemically inert mesh (FCNet) into the polymer layer via a second FCP-application (Fig. 2), (3) performing three VASE measurements at different locations on the sample, and (4) storing the sample in a desiccator maintained at <10%-to-18% RH until the designated time for next layer of FCP to be applied. The samples were left in the laboratory environment for 1-to-3 h per ellipsometry measurement and 2-to-6 h per AFM measurement (Utah air is dry-RH typically <30%, maximum ~50%). Typically, the formulations were applied for at least 30 min before polymer removal, but there were a couple of occasions where we left the samples with polymer applied on them in the RH <10%-to-18% desiccator storage. The desiccator storage RH was typically <10% but did rise to about 18% for a small period of time (about a week) during the study.

B. Variable-angle, spectroscopic ellipsometry

A J.A. Woollam RC-2 variable-angle, spectroscopic ellipsometer uses an ~1 mm diameter beam spot. At higher incident angles



FIG. 2. One of the four FCP-applied samples with mesh applied on a paper towel. After the initial FCP layer had dried, the chemically inert mesh tab was placed near an edge as shown. A second FCP layer was applied on the upper left corner where the mesh tab is located to ensure the mesh tab would be embedded in the FCP layer.

(around 75°), the beam spot would be stretched into an ellipse with a major axis of 6 mm and a minor axis of 1 mm. Each sample was measured in three different locations on the surface such that the beam spot would remain on the sample to assess variations across the surface and get average thickness values across the full sample. The angles of incidence tested are 50°–80° in 5° increments with an acquisition time of at least 5 s. After data collection, the measurements were processed using J.A. Woollam's CompleteEase software to model the subangstrom thicknesses of Al_2O_3 , LiF, and Al, as described in Sec. III.

C. Tapping-mode atomic force microscopy

To determine (1) the height, width, and shape of features that might be formed after FCP-application and (2) changes in root mean square of surface height irregularities (RMS roughness), we used a Dimension V 5100 AFM with ~300 kHz tapping-mode tip probes to image topographical maps of the surface. During the first measurements, we took three $4 \times 4 \mu\text{m}^2$ scans and one $10 \times 10 \mu\text{m}^2$ scan each with 1024×256 pixels in locations with no visible features was recorded at a scan frequency of 0.5 Hz to ensure high resolution. All future measurements, we adjusted to three $5 \times 5 \mu\text{m}^2$ scans and one $10 \times 10 \mu\text{m}^2$ scan with the same parameters. Gain parameters and amplitude setpoint were chosen to avoid artificial streaking resembling a “comet tail.” Typically, for a feature larger than 50 nm, higher integral gain and proportional gain parameters are required. Generally, we chose an integral gain and proportional

04 June 2025 14:57:01

gain of 0.3 and 0.6, respectively, for rougher images and 0.15 and 0.225, respectively, for flat images. Initially, we used 0.15 and 0.2, respectively, for flat images but adjusted as time went on. The integral gain and proportional gain were increased if the features were not fully resolved. The proportional gain was generally set 1.5–2 times greater than the integral gain. The amplitude setpoint, which determines the force on the tip probe in tip-surface interaction and typically around 300–400 mV, was reduced by 10% at the beginning of each measurement and adjusted in 10 mV steps if necessary.

Each measurement was recorded as raw data that need to be flattened, processed to remove artifacts, and analyzed. We utilized the capabilities of open-source, AFM processing software GWYDDION¹⁷ to process the raw data to observe surface features and RMS surface roughness. Features significantly larger (>50 nm difference) than the rest of the nanostructure, however, would obscure the nanoroughness, so the features needed to be filtered out to obtain the RMS roughness. When observing nanoroughness, we blended large features using either a Laplace correction or a Laplace-Fractal blend correction with the surrounding nanostructure.

III. MODELING

VASE requires specific modeling techniques to prevent fitting errors. A correlation problem, for example, can cause the fit to confuse two thicknesses with each other. This usually occurs when the total of the individual optical thicknesses—defined as the product of the refractive index and the film thickness—is much less than the wavelength of light, and the materials have similar dispersion. Dielectric thicknesses less than 10 nm can be degenerated due to this problem.¹⁸ Similar dispersion curves—defined as the refractive index as a function of photon energy—in particular contribute to this class of correlation difficulties. In this study, the derived LiF, AlF₃, and Al₂O₃ optical layer thicknesses were strongly correlated. To prevent nonsensical thicknesses due to correlation, we adopted a two-step fit procedure. In the first step, we (1) constrained the surface roughness with AFM measurements and (2) fit the thickness of the next three layers (LiF, AlF₃, and Al₂O₃) as one “apparent” LiF layer. As part of the first-stage fitting, we also fit the Al layer thickness. Decreasing trends in the Al thickness were assumed to be associated with alumina growth from oxidation, as we found in Sec. IV. We used such decreases in the Al thickness to calculate the Al₂O₃ thickness that may have formed using this process: 1 nm of Al disappear yields about 1.54 nm of oxide [see Eq. (2)] as shown below.

A. Constraining roughness

CompleteEase defines roughness as a Bruggeman effective medium approximation layer¹⁹ between the top-most layer and a void layer. This roughness is represented by a thickness value while the RMS surface roughness as measured by AFM is represented by the RMS of surface height variations. Therefore, we assumed the thickness could be approximated as a box with an area of 1 and height of a Gaussian with standard deviation equal to the average RMS roughness. We determined that the resulting conversion factor of 2.51, as shown in Eq. (1), would be used to convert the AFM-measured RMS roughness σ to VASE-constraint roughness

thickness x_r ,

$$x_r = 2.51\sigma. \quad (1)$$

In the case that there was no corresponding roughness value with a VASE measurement, the previously recorded VASE-constraint roughness thickness was used to constrain the roughness. Therefore, any changes in the top-most layer—in this case, LiF—may indicate that there is increasing or decreasing roughness.

B. First-stage model fit

As discussed above, the total optical thickness for the three dielectric layers, LiF, Al₂O₃, and AlF₃, is small compared to the wavelength of light, and their indices are sufficiently similar that the thickness values calculated from fitting two or three of the three layers at the same time cannot be relied upon to yield accurate results. To prevent these errors due to correlation, the LiF, Al₂O₃, and AlF₃ thicknesses were fit as a single “apparent” LiF thickness. LiF was used since it is the thickest of the three. The optical constants we used were a Sellmeier fit to Pallik’s LiF provided by Woollam’s CompleteEase.²⁰ As for the Al layer, we utilized an 8-oscillator Gen-Osc model. Each oscillator was parameterized to determine the Al optical constants shown in Fig. 3.

C. Second-stage and final model fit

Once the initial fit was performed, we used the observed decrease in the Al thickness to calculate the Al₂O₃ thickness increase based on stoichiometry supposing the oxide was β -alumina ($\rho = 3.31 \text{ g/cm}^3$) rather than corundum/sapphire ($\rho = 4.0 \text{ g/cm}^3$).²¹ We used the atomic layer deposited alumina layer described in the work of Shah *et al.* for optical constants.²² In particular, we used their Sellmeier model values. We had assumed that

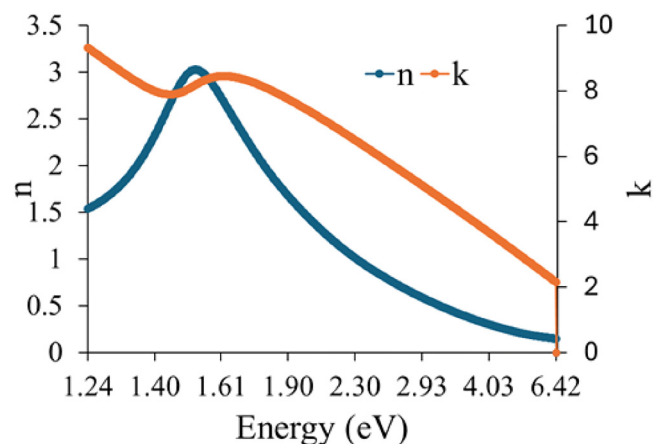
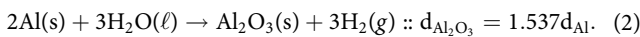


FIG. 3. Optical parameters used to model the aluminum layer thicknesses. These were parameterized specifically for the Al + XeLiF thin-film stack, as described in Sec. III B.

04 June 2025 14:57:01

the reaction was occurring between water molecules and the aluminum surface, whose result is shown in Eq. (2). This allows the Al_2O_3 thickness to be estimated as a function of Al thickness lost. This inferred Al_2O_3 thickness was used to constrain the Al_2O_3 thickness to give an estimate of the Al_2O_3 increase during the FCP treatment. There is only one parameter left for the films above the aluminum in the model is left to be fit, that is, the LiF layer thickness. One possible reaction is



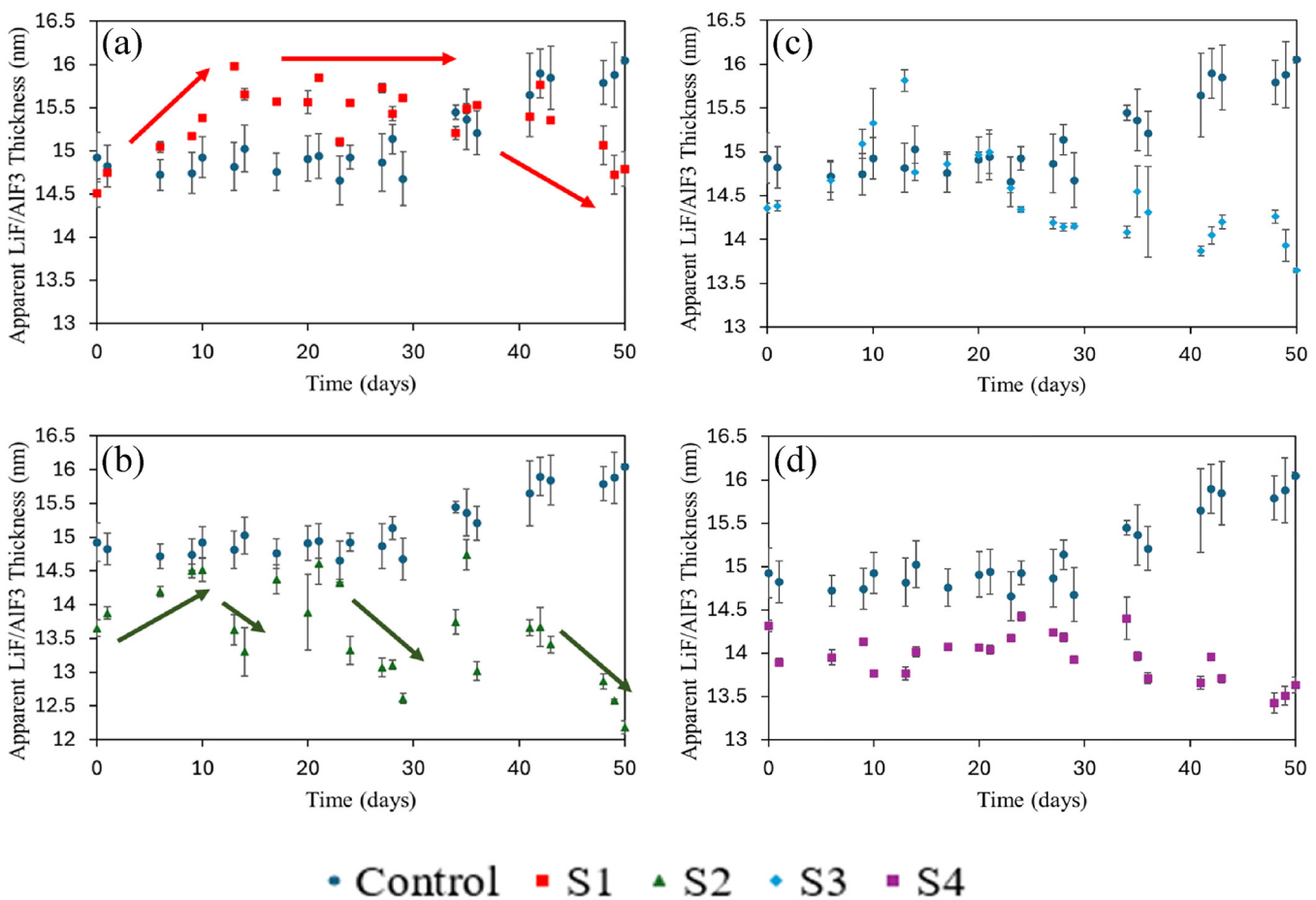
IV. RESULTS AND DISCUSSION

As we applied FCP, we observed two formulations—S1 and S3—peeled off an about 1 mm spot of the Al + XeLiF stack at

different times in the 50 day trial. No other apparent visible damage was observed from the samples. We performed VASE (Sec. IV A) and AFM three times on all the samples in this study (Sec. IV A), UV reflectance measurements once on three of the four formulation-applied samples (Sec. IV B), and x-ray photoelectron spectroscopy (XPS) (Sec. IV C) on two of the samples a couple months after the application tests were completed.

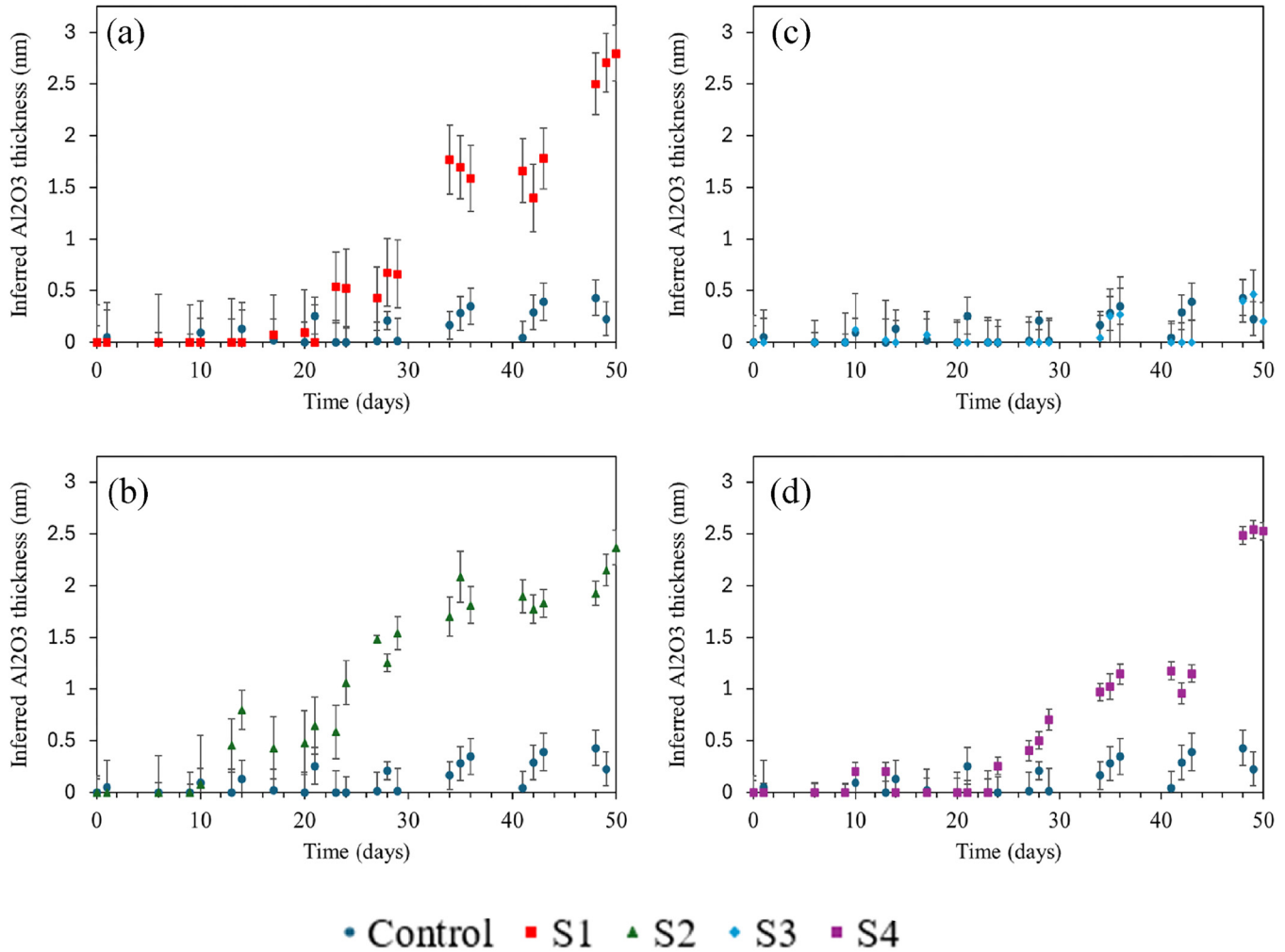
A. VASE trends for repeated applications

There is an increase in the apparent LiF thickness for three of the four formulations tested for the first 2 weeks (Fig. 4). This increase is likely due to an increase in roughness (see Sec. IV D). S2 and S3 experienced a decrease while S1 stayed constant until it decreased back to its initial state. It should be noted that S1 was



04 June 2025 14:57:01

FIG. 4. LiF thickness of XeF_2 -passivated LiF on Al (XeLiF) according to VASE. Each data point was taken after the application and removal of one of four current formulations of First Contact Polymer (FCP). (a) S1, (b) S2, (c) S3, and (d) S4. Each data point corresponds to a set of three ellipsometric measurements across one of the $1 \times 1 \text{ in.}^2$ samples. The colored left-to-right arrows are to guide the eye. The uncertainty is determined based on the standard error of the measurements. Measurement angles were from 50° to 80° in 5° increments over the 190–1000 nm wavelength range. As the thickness is only apparent, any change above the Al_2O_3 layer would be reflected by this thickness. Apparent LiF increases may represent changes in the LiF layer, the roughness (i.e., changes not observed by AFM), or anything else above the Al_2O_3 layer. Any decrease would lead to increased smoothness not captured by the AFM or removal of some feature on top. At 34 days, the sample with formulation S1 was unintentionally contaminated with water.

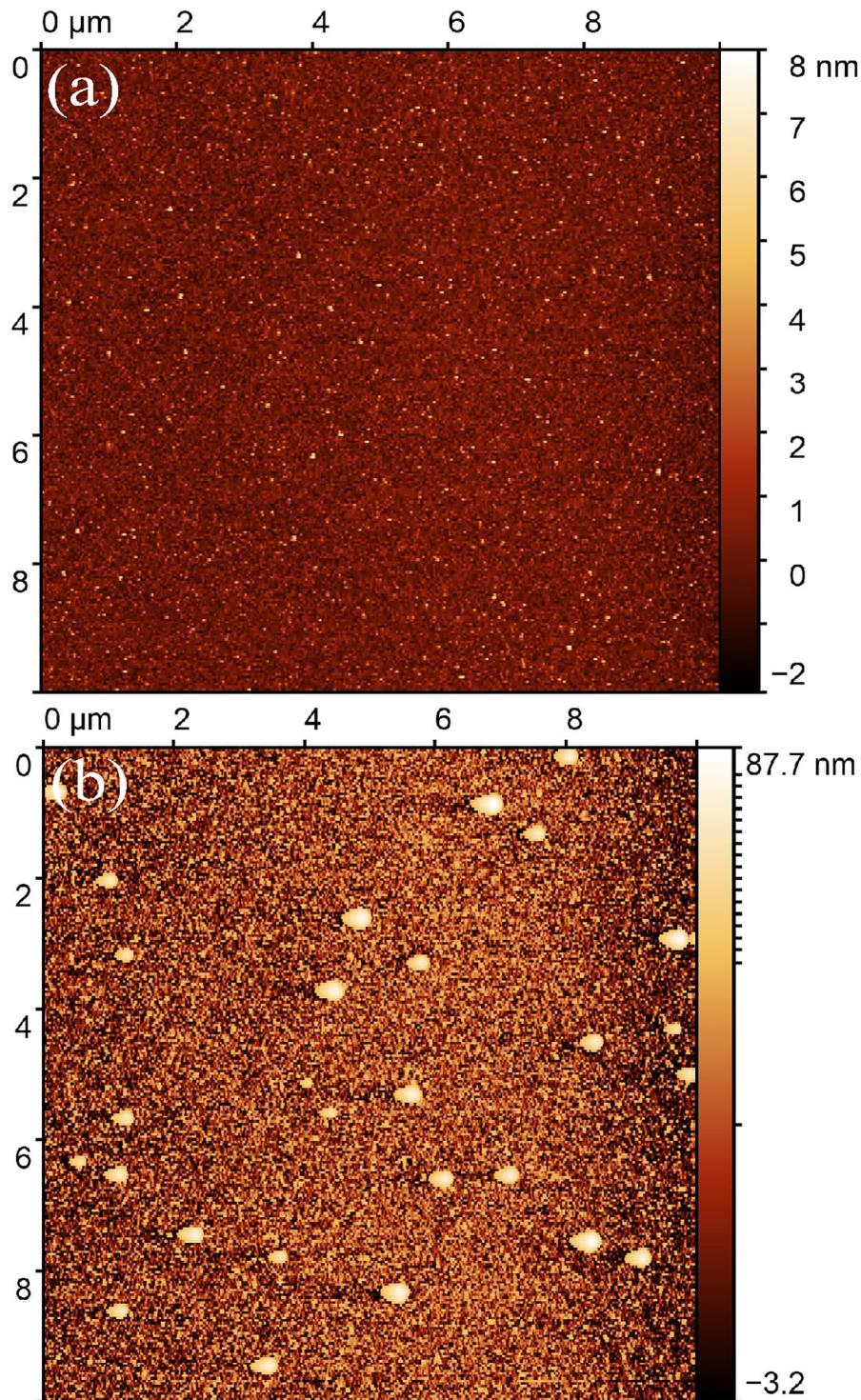


04 June 2025 14:57:01

FIG. 5. Al_2O_3 thickness of XeF_2 -passivated LiF on $(\text{Al} + \text{XeLiF})$ as calculated from VASE data using CompleteEase. Each data point was taken after the application of one of the four current formulations of First Contact Polymer (FCP). (a) S1, (b) S2, (c) S3, and (d) S4. Each figure also has plotted for comparison the data measured from a control sample at the same peel-off count as the coated samples. Each data point corresponds to three measurements across $\sim 1 \times 1 \text{ in.}^2$ samples with measurement angles of 50° – 80° from 190 to 1000 nm. The “error bars” shown were also calculated from the standard error of the modeled thickness values from the three measurements of each point. All formulations appeared to be removed without any increase to the Al_2O_3 layer. S1, S2, and S4 saw a considerable increase when compared with the control after repeated applications. S3 remained consistent with the control, which shows S3 is a promising candidate for cleaning XeLiF_2 . At 34 days, S1 was unintentionally contaminated with water, which accounts for the increase.

TABLE I. AFM RMS roughness results of the formulation-tested samples before FCP-repeated treatment, after the first application of FCP, and after five to six cycles. From the first application, S1 and S3 were found not to increase the roughness. After five to six applications, which is much more cleaning than necessary, only S3 was able to be used without roughening above 1 nm RMS. S1 appears to do so as well, but features formed on the surface shown in Fig. 6.

Application number	S1 RMS roughness (nm)	S2 RMS roughness (nm)	S3 RMS roughness (nm)	S4 RMS roughness (nm)	Control RMS roughness (nm)
0	0.64	0.69	0.76	0.89	0.75
1	0.69	1.02	0.64	1.1	0.87
5–6	0.78	1.23	0.81	1.18	0.94



04 June 2025 14:57:01

FIG. 6. AFM micrographs of XeLiF (a) before and (b) after six FCP-applications of formulation 2. Small dome-like features were observed on the surface of Al + XeLiF that were not observed before FCP-application. These are the "white spots" on the figure on the right. Note that the white spots are about 20–90 nm high and about 200 nm across, making them shallow features. Note that in (b), a logarithmic scale is used for height instead of a linear one as used in (a).

inadvertently contaminated with water at around 34 days, as shown in Fig. 5. The contamination of S1 is more apparent for the oxide thickness, as there is a 1 nm increase in the Al₂O₃ thickness.

The cleaning of Al+XeLiF requires at least one FCP-application. A successful FCP cleaning requires that particulate/molecular contaminants are removed and that the coatings are not damaged by the processing. An increase in roughness would reveal that the formulation damaged the coatings. Based on current understanding of the aging of LiF films where humidity is present,⁷⁻¹⁰ LiF films eventually roughen probably due to Oswald ripening. The apparent LiF thickness may increase due to water adsorbed on the film surface and in micropores being measured as part of the film by VASE. LiF is slightly soluble in water. Water can catalyze grain growth, atoms from small grains' preferential dissolving due to their higher surface energy and redepositing on larger grains due to their lower surface energy. Thus, large grains grow even larger at the expense of the film's integrity. The neighborhood of larger grains constitutes pores, allowing more water to condense by capillary action (Laplace pressure), accelerating this roughening. For a water surface in a pore with a negative meniscus, the Laplace pressure as given by the Kelvin equation can be very large, ensuring the pores fill with some water from the air. In this scenario, water transferred from any source including a cleaning formulation onto the film surface could assist the degradation process. It is reasonable to speculate that this surface roughening could increase with time or peel-off cycles. In Table I, the RMS roughness as measured by AFM for the first few peel-offs is

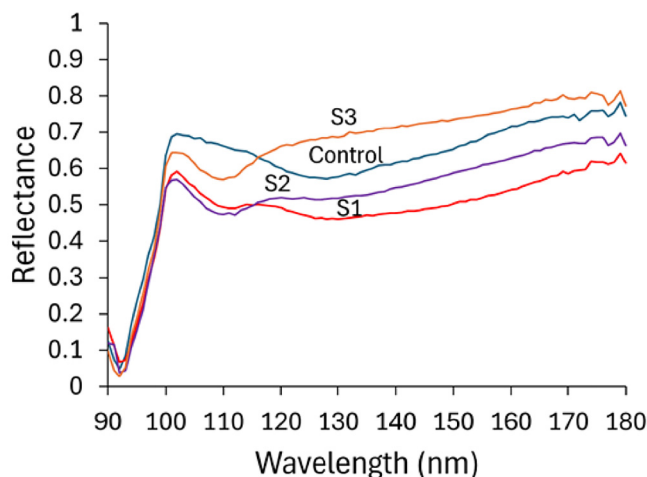


FIG. 7. Far-UV reflectance of Al+XeLiF, including a control sample with no FCP applied and curve measured for the XeLiF three different formulations (S1, S2, and S3) each applied multiple times. Note that the S3 sample maintains high FUV reflectance. These semitransparent Al+XeLiF samples are not expected to reach the same high reflectance as the opaque Al+XeLiF coatings used for HWO, so the control represents what the samples are like without any FCP applied. Surface plasmon excitations can reduce reflectivity from the 130-to-150 nm range (Ref. 7). There is a dip at 110 nm for all the FCP-applied samples, which will be subject to further research. S3 retained the highest reflectance of the three FCP-applied samples.

shown. Roughening is seen in all cases including the control sample that was never cleaned.

A single FCP-application and removal did not significantly affect the sample for three of the four FCP formulations other than cleaning it. However, small dome-shaped features (about 20–90 nm high, 150–200 nm wide) were observed on S4 after the first peel-off. However, these were not seen after subsequent peel-offs. The identity

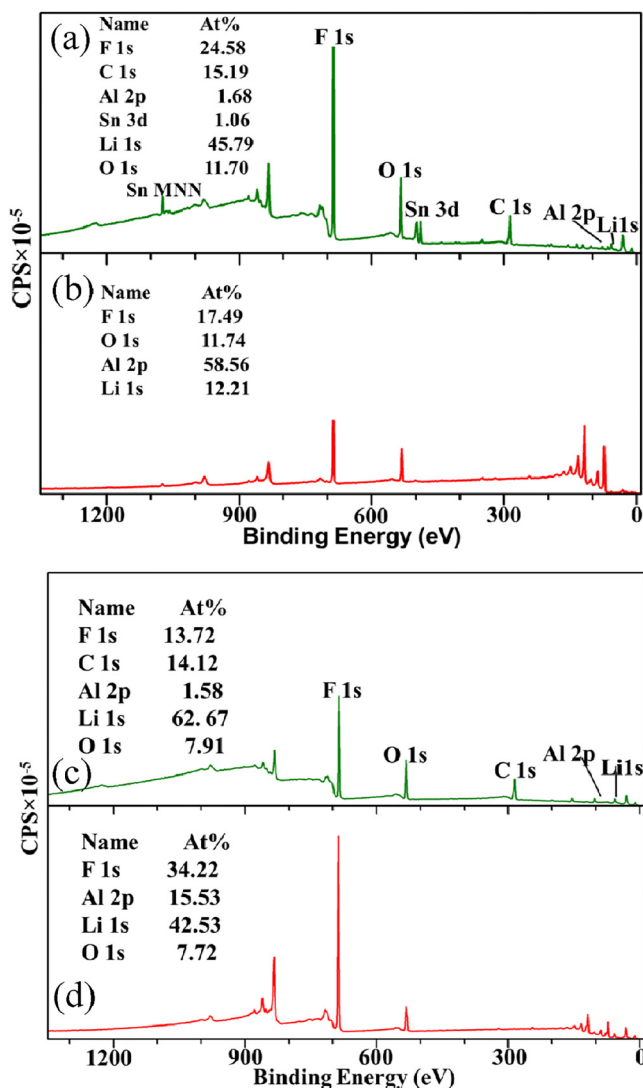


FIG. 8. Survey scan of the (a) formulation S2-cleaned and (c) scans of the control at the surface and [(b) and (d)] at the AlF₃ and Al interface after around 20 sputter cycles from the surface. CPS stands for "Counts per second." On the surface, we observed F 1s, C 1s, Al 2p, Li 1s, and O 1s signals on both the FCP-applied sample and the control. On the FCP-sample, there was a Sn 3d signal at about 1.0 at. %, which differentiated it from the control. This signal has been observed before on samples cleaned by certain FCP formulations (Ref. 23). At the AlF₃ and Al interface, we observed an F 1s, O 1s, Al 2p, and Li 1s signal.

04 June 2025 14:57:01

of the features could not be determined via AFM. Possible hypothetical sources of these features could be that they are submicrometer particulates that adhered to the surface after FCP-applications, FCP residue (generally no residue has ever been seen on any surfaces with FCP in the past), or the agglomeration of the LiF into clumps. Localized delamination of Al + XeLiF from the substrate as was observed by Lewis in small, localized regions is also possible.¹⁰

As shown in Fig. 6, we observed these features in S1 and S2. Subsequent peel-offs, however, caused dome-shaped hillocks to form again on the Al + XeLiF samples. After 5–6 peel-offs, 20–90 nm high and 200 nm wide dome-like features were observed to have formed on the surface. However, if they were from the FCP directly, the depolarization of the associated ellipsometric analysis would substantially increase. This was not observed in VASE measurements. The composition of the hillocks is unknown until further investigations are made.

B. UV reflectance

Near the end of the study, we measured the UV reflectance of formulation S1, S2, S3, and the control at NASA-GSFC from 90 to 180 nm (Fig. 7). As the aluminum layer in the sample is not optically thick enough to completely reflect the light, the sample cannot be expected to reach HWO performance levels. While these samples are from the same batch of thin Al + XeLiF samples from the work of Quijada *et al.*,⁶ the control exhibited a large dip around 130 nm not present in typical Al + XeLiF samples nor seen in Ref. 6. The initial sample reflectance was expected to vary 5%–10% from each other based on Al thickness variation since Al was semi-transparent. The dip around 130 nm in both S1 and the control is often attributed to surface plasmon excitation caused by increased roughness on the sample surface.⁷ This lower-than-expected reflectance can, therefore, be attributed to losses from surface damage the control sustained during transit and handling while at BYU and is not observed in standard Al + XeLiF samples. We did not observe oxidation from the ellipsometry results, so the decrease is not likely to be oxidation. In addition, the AFM results of the control showed that the surface morphology changed slightly about 14 days. This change in surface morphology could be attributed to submicrometer dust from the lab environment or surface damage. The change in surface morphology was not apparent in the ellipsometry but could explain the surface plasmon excitation. Of important note, there is a dip around 110 nm present in S1, S2, and S3 that is not observed from the control nor other samples. This dip will be the subject of future research.

C. X-ray photoelectron spectroscopy

After the series, the samples were left without FCP-application and stored in the desiccator. Two to three months after the 50-day study, we examined the elemental composition of the surfaces of samples S2 and the control via XPS. As S2 had bump-like features on it, the surface scans help clarify the feature composition.

XPS was performed with monochromatic Al K α x rays (Thermo Scientific, Waltham, MA, USA). After the initial survey and narrow scans were collected, additional scans were collected following sputter etching with a monoatomic Ar⁺. Each sample underwent a total of 19 etch cycles. The data were analyzed using

CASAXPS software (Casa Software Ltd., Teignmouth, Devon, UK). We analyzed S2 and the control. To prevent the samples from absorbing water vapor from the air due to hygroscopicity of LiF, the samples were kept in a transport desiccator calibrated with a humidity sensor that typically read 11% relative humidity.

The first survey scan of S2 indicates the presence of Sn 3d, C 1s, Al 2p, O 1s F 1s, and Li 1s. After the 19th etch cycle, only Al 2p, O 1s F 1s, and Li were present on the surface as shown in Figs. 8 and 9. Sn 3d peaks were also seen in the first scan as shown in Ref. 10. The presence of Sn on FCP cleaned surfaces has been noted in other reports.²³ We note that the relative amount of Sn is small, about 1%, and vanished after the first sputter etch.

Does FCP leave residue on the surface beyond the minor amounts of Sn? To answer this question, we considered what the

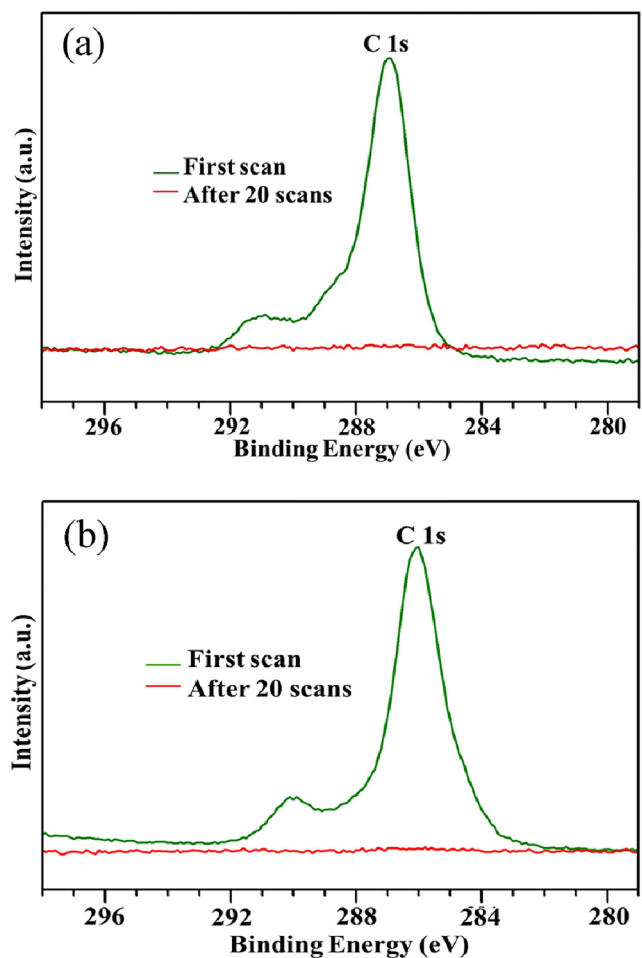


FIG. 9. Carbon narrow scan of the (a) formulation S2 applied sample and (b) control at the surface (first scan, labeled C 1s) and near the interface of the AlF₃ and Al layer (shown beneath the surface scan) after 20 sputter cycles. Similar quantities of carbon suggest that no residual FCP adhered on the surface at the time of the XPS scan.

04 June 2025 14:57:01

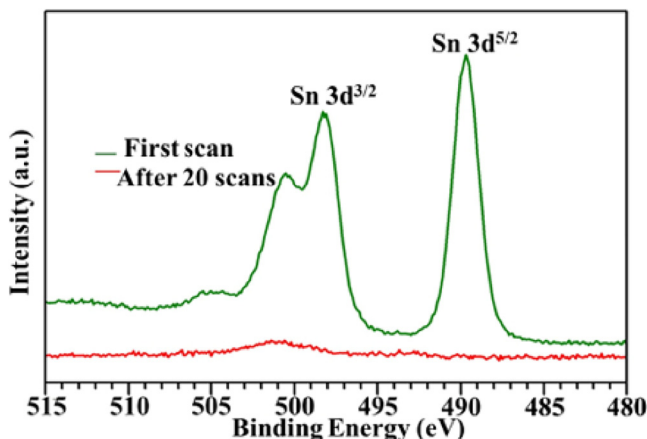


FIG. 10. Tin presence as a minor constituent on the surface of surface treated with S2. Narrow scan of the S2 applied surface scan at position of tin photoelectrons generated by XPS (Al $K\alpha$) on the surface (first scan, labeled Sn signals) and near the interface between AlF_3 and Al (shown beneath the surface scan). The Sn signal is only found on the surface of the sample and was previously observed in other research using FCP (Ref. 23).

residuals would likely leave. Any polymer that adheres to the surface would likely show an increased C peak. To answer this question, we compared the S2 formulation-applied sample with the control (see Fig. 9). Both surfaces had nearly the same quantity of carbon. As FCP had not been applied to these samples for some time, the adventitious carbon redeposited on the surface of the S2 applied sample. As the carbon signals are so identical, it is likely that negligible amounts of FCP adhered to the surface.

D. Discussion

We have observed notable changes in the samples, but what do they signify? We classify the effectiveness of the four FCP formulations based on the following criteria: (1) Did the apparent LiF thickness increase significantly after a single application compared with the first measurement? (2) Was the RMS roughness after a single application greater than 1 nm RMS roughness, as needed for coronagraphy?¹⁵ (3) Did the apparent LiF thickness change significantly from the control after repeated application? (4) Did the inferred Al_2O_3 thickness increase after repeated application compared with the control? (5) Was the RMS roughness after 5–6 peel-offs greater than 1 nm RMS roughness? (6) Was there significant carbon residuals from the FCP? The results answering criteria 1 through 4 are summarized in Tables II and III. Sample S2 was found to not have significant carbon increase when compared with the control, so it is unlikely that any FCP was left behind, answering criteria 6 for this formulation.

For a single cleaning, S1 and S3 did not affect the LiF, roughness, or oxidation. For repeated cleaning, we observed that the S3-treated sample had the highest reflectivity, most constant and low roughness, and no significant aluminum oxidation. We also observed that S4 had a more consistent decrease in LiF thickness. Knowing the difficulties related to FCP-application based on

TABLE II. Summary of the results presented in this paper corresponding to a single FCP-application. The second column notes what the overall trend in the apparent LiF thickness found by ellipsometric analysis was. The third column indicates whether the formulation oxidized the sample more than the control got oxidized. The fourth column indicates whether there was an increase in roughness that surpassed the 1 nm RMS limit set for coronagraphy (Ref. 15).

Formulation	LiF	Oxidation	Roughness
S1	No significant difference	No significant difference	Did not surpass 1 nm RMS
S2	No significant difference	No significant difference	Surpassed 1 nm RMS
S3	No significant difference	No significant difference	No significant difference
S4	Slight decrease	No significant difference	Surpassed 1 nm RMS

formulation properties is essential to understand the possible formulation difficulties.

It can be seen that two formulations—S1 and S3—could be applied to the surface without significant roughening or growth of apparent LiF and Al_2O_3 . This is a noteworthy observation, suggesting that the FCP formulations can work well with the Al + XeLiF coating for at least a single cleaning without damaging the surface. If the mirrors are to be cleaned multiple times by FCP-application, one of the formulations—S3—was observed to not cause significant roughening or layer growth. This indicates that formulations like S3 can be used multiple times without changing the Al + XeLiF surface significantly. The features found on S1 and S2 surfaces by AFM may be film delamination, film blistering, or small globules of aluminum oxide (hydroxide) where AlF_3 has become thin.^{7–10} We have observed LiF clustering in the past, so this may also be the cause.^{8,9} Nevertheless, since the mirror reflectance appears high, XPS results (see Fig. 11) do not show evidence of such features. Perhaps, the most important result from this work is that the high far-UV reflectance that Al + XeLiF is known for remained high (with the exception of the 110 nm dip subject to further research).

TABLE III. Summary of the results presented in this paper corresponding to repeated FCP-applications. The second column notes the overall trend in LiF over the peel-off trials. The third column notes the oxidation of the aluminum with peel-off counts. The fourth column indicates whether the roughness of the film went above 1 nm RMS after six peel-offs.

Sample	LiF	Oxidation	Roughness
S1	Variation	Significant increase	Did not surpass 1 nm RMS
S2	Variation	Significant increase	Surpassed 1 nm RMS
S3	Variation	No significant increase	Did not surpass 1 nm RMS
S4	Slight decrease	Significant increase	Surpassed 1 nm RMS

04 June 2025 14:57:01

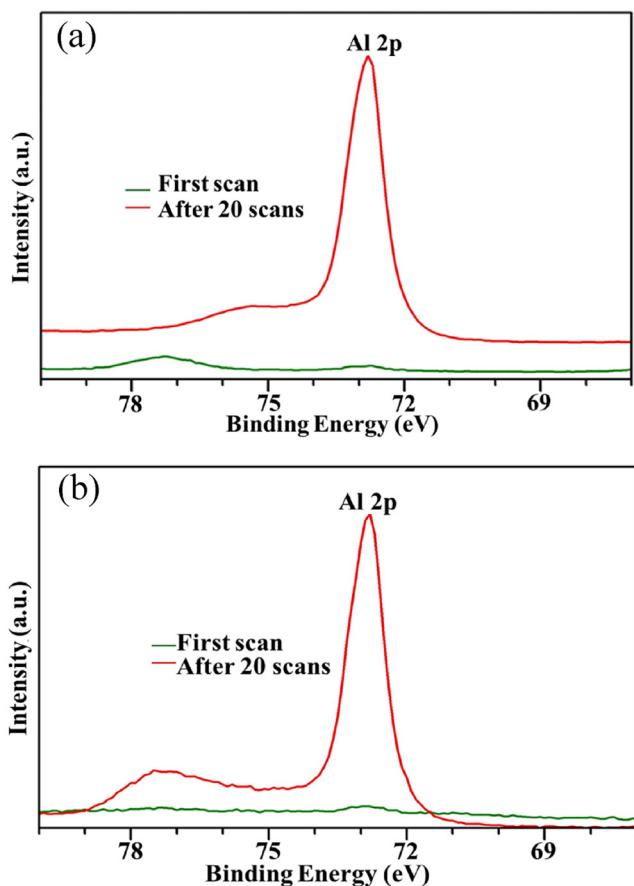


FIG. 11. Narrow XPS scan of the (a) S2 applied sample and (b) control (S5) at the position of Al photoelectrons. Both graphs feature a surface scan (first scan) and at the interface of AlF_3 and Al (after 20 scans—labeled Al 2p). There is the presence of aluminum that is oxidized signal to the left on the Al 2p peak in the control. The peak at 77 eV in the control sample is evidence of aluminum oxidation.

V. SUMMARY AND CONCLUSIONS

In our 50-day study, we investigated the effect of applying FCPs repeatedly to Al + XeLiF samples. Four different FCP formulations were investigated. We observed no substantial increase in the Al_2O_3 thickness for one of the FCP formulations, S3, after 23 applications. The only notable problem with S3 was the ~ 1 mm spot of Al + XeLiF that was removed after multiple peel-off cycles. The formulation also did not produce a substantial increase in surface RMS roughness after five applications and no apparent features formed on the surface. The Al_2O_3 thickness also did not substantially increase after the 23 application-removal cycles. Another formulation—S4—did not appear to cause substantial increases to the apparent LiF thickness, indicating no detectable roughening to XeLiF by ellipsometry.

We saw 20–90 nm high, 200 nm wide clumps formed on the surface of two of the four samples—S1 and S2. XPS analysis

showed no substantial increase in carbon deposited on the surface after the experiment, so the bumps are not FCP residue. In addition, ellipsometric depolarization did not substantially increase, meaning that the features did not significantly increase scattering from the sample during ellipsometry measurement. The features, therefore, are likely blistering from excessive polymer-to-surface adhesion or LiF coalescing on the surface of the Al + XeLiF samples. The coalescing may be caused by the interaction between the water inside FCP and Al + XeLiF causing a restructuring of the surface. A new FCP formulation tailored to Al + XeLiF could be created, which cleans and protects the surface without significantly altering LiF.

ACKNOWLEDGMENTS

We acknowledge funding from the NASA Goddard (Contract No. 80NSSC23K0546), NASA SBIR funding for this work (Contract No. 80NSSC24PB405), and the NSF REU grant for Drew Watson's work (NSF Grant No. 2348770). The authors gratefully acknowledge J.A. Woollam Co., Inc. providing several 1-year licenses for the CompleteEase software. This allowed us to analyze the many Ψ and Δ files this study generated. This work has been supported by the Department of Physics and Astronomy and the College of Computation, Mathematics and Physical Sciences, Brigham Young University. We thank Manuel Quijada, Javier del Hoyo, Edward Wollack, and Mateo Batkis at NASA Goddard as well as Luis Rodriguez de Marcos at the Catholic University of America for providing the Al + XeLiF samples used in this study. Luis Rodriguez de Marcos also performed the reflectance measurements shown in this paper. OpenAI's ChatGPT-4o was used to proofread the grammar and flow of the paper, although the authors wrote the entirety of the paper. We also thank Edward Wollack at NASA Goddard for providing feedback regarding the manuscript.

04 June 2025 14:57:01

AUTHOR DECLARATIONS

Conflict of Interest

James Hamilton is the CEO of Photonic Cleaning Technologies, which produces and sells First Contact Polymer.

Author Contributions

Joshua Vawdrey: Conceptualization (equal); Data curation (supporting); Formal analysis (lead); Investigation (lead); Methodology (equal); Project administration (equal); Visualization (equal); Writing – original draft (lead); Writing – review & editing (lead). **James Hamilton:** Funding acquisition (lead); Resources (lead); Supervision (equal); Writing – review & editing (equal). **Drew Watson:** Investigation (equal). **Lauren Miner:** Investigation (equal). **Osemudiamhen Destiny Amienghemhen:** Investigation (equal); Writing – original draft (supporting). **Walter Paxton:** Investigation (supporting); Supervision (supporting). **David Allred:** Formal analysis (supporting); Funding acquisition (equal); Investigation (supporting); Methodology (supporting); Supervision (lead); Writing – review & editing (equal).

DATA AVAILABILITY

The data that support the findings of this study are available from the corresponding author upon reasonable request.

REFERENCES

- ¹C. Burrows, NASA Technical Report No. NASA-CR-189751, Space Telescope Science Institute, Baltimore, MD, 1990.
- ²E. M. Stewart, *Proc. SPIE* **10748**, 16 (2018).
- ³D. M. Lewis, C. M. Plewe, A. G. Stapley, J. J. Vawdrey, R. S. Turley, and D. D. Allred, *Proc. SPIE* **11451**, 271 (2020).
- ⁴B. Fleming *et al.*, *Appl. Opt.* **56**, 9941 (2017).
- ⁵M. A. Quijada, L. V. Rodriguez de Marcos, J. G. Del Hoyo, E. Gray, E. J. Wollack, and A. Brown, *Proc. SPIE* **12188**, 66 (2021).
- ⁶M. A. Quijada, J. G. Del Hoyo, L. V. Rodriguez de Marcos, E. J. Wollack, M. F. Batkis, D. M. Lewis, T. D. Rydalch, and D. D. Allred, *Proc. SPIE* **13093**, 152 (2024).
- ⁷D. M. Lewis, T. D. Rydalch, D. D. Allred, L. Rodriguez de Marcos, M. A. Quijada, J. del Hoyo, and M. Batkis, *Proc. SPIE* **13100**, 20 (2024).
- ⁸T. D. Rydalch, D. M. Lewis, and D. D. Allred, *Proc. SPIE* **12188**, 207 (2021).
- ⁹T. Rydalch, “Stability and oxidation of Al mirrors coated with Xe-passivated LiF thin films,” B.S. thesis (Brigham Young University, 2024), see <https://physics.byu.edu/docs/thesis/1701>.
- ¹⁰D. M. Lewis, “Stability of LiF mirror coatings on space telescopes at L2 orbit,” M.S. thesis (Brigham Young University, 2025), see <https://scholarsarchive.byu.edu/etd/10625>.
- ¹¹J. J. Vawdrey, J. P. Hamilton, and D. D. Allred, *Proc. SPIE* **12666**, 1266609 (2023).
- ¹²M. H. Phelps, K. E. Gushwa, and C. I. Torrie, *Proc. SPIE* **8885**, 88852E (2013).
- ¹³J. Tumlinson *et al.*, “Unique astrophysics in the Lyman ultraviolet,” [arXiv:1209.3272](https://arxiv.org/abs/1209.3272) (2012).
- ¹⁴L. D. Feinberg, J. Ziemer, M. Ansdell, J. Croke, C. Dressing, B. Mennesson, J. M. O’Meara, J. Pepper, and A. Roberge, *Proc. SPIE* **13092**, 59 (2024).
- ¹⁵H. P. Stahl, *Proc. SPIE* **12676**, 25 (2023).
- ¹⁶J. A. Woollam, B. D. Johs, C. M. Herzinger, J. N. Hilfiker, R. A. Synowicki, and C. L. Bungay, *Proc. SPIE* **10294**, 1029402 (1999).
- ¹⁷D. Nečas and P. Klapetek, *Open Phys.* **10**, 181 (2012).
- ¹⁸H. G. Tompkins and J. N. Hilfiker, *Spectroscopic Ellipsometry: Practical Application to Thin Film Characterization* (Momentum, New York, 2016).
- ¹⁹D. A. G. Bruggeman, *Ann. Phys.* **416**, 636 (1935).
- ²⁰E. D. Palik and W. R. Hunter, “Lithium fluoride (LiF),” in *Handbook of Optical Constants of Solids*, edited by E. D. Palik (Academic, San Diego, CA, 1997), p. 675.
- ²¹P. Villars, “ β -alumina (NaAl₁₁O₁₇) crystal structure: Datasheet,” in *PAULING FILE Multinaries Edition - 2022* (Springer Materials, Heidelberg, 2011). See https://materials.springer.com/isp/crystallographic/docs/scd_1410950.
- ²²D. Shah, D. I. Patel, T. Roychowdhury, D. Jacobsen, J. Erickson, and M. R. Linford, *Surf. Sci. Spectra* **26**, 026001 (2019).
- ²³Kratos Analytical, Ltd., AZoM Report, 2019.